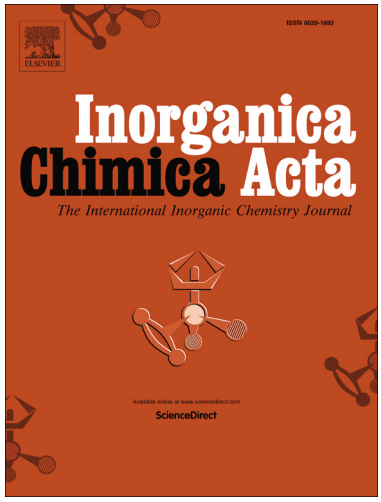

Research paper

Catalytic Epoxidation using Dioxidomolybdenum(VI) Complexes with Tridentate Aminoalcohol Phenol Ligands

Md. Kamal Hossain, Jörg A. Schachner, Matti Haukka, Nadia C. Mösch-Zanetti, Ebbe Nordlander, Ari Lehtonen

PII: S0020-1693(18)30919-8
DOI: https://doi.org/10.1016/j.ica.2018.10.012
Reference: ICA 18558

To appear in: *Inorganica Chimica Acta*

Received Date: 15 June 2018
Revised Date: 8 October 2018
Accepted Date: 8 October 2018

Please cite this article as: d.K. Hossain, J.A. Schachner, M. Haukka, N.C. Mösch-Zanetti, E. Nordlander, A. Lehtonen, Catalytic Epoxidation using Dioxidomolybdenum(VI) Complexes with Tridentate Aminoalcohol Phenol Ligands, *Inorganica Chimica Acta* (2018), doi: https://doi.org/10.1016/j.ica.2018.10.012

Catalytic Epoxidation using Dioxidomolybdenum(VI) Complexes with Tridentate Aminoalcohol Phenol Ligands

Md. Kamal Hossain,[a] Jörg A. Schachner,*[b] Matti Haukka,[c] Nadia C. Mösch-Zanetti,[b] Ebbe Nordlander,*[a] and Ari Lehtonen*[d]

a. Chemical Physics, Department of Chemistry, Lund University, P.O. Box 124, SE-221 00 Lund, Sweden
b. Department of Chemistry, University of Graz, Schubertstraße 1, 8010 Graz, Austria
c. Department of Chemistry, P.O. Box 35, University of Jyväskylä, FI-40014 Jyväskylä, Finland
d. Inorganic Materials Chemistry Research Group, Laboratory of Materials Chemistry and Chemical Analysis, Department of Chemistry, University of Turku, 20014, Turku, Finland

***** Corresponding author
E-mail address:
Ari.Lehtonen@utu.fi (A. Lehtonen)
Ebbe.Nordlander@chemphys.lu.se (E. Nordlander)

Dedicated to Rabindranath Mukherjee on the occasion of his 65th birthday, and in recognition of his outstanding contributions to coordination chemistry and bioinorganic chemistry

Abstract

Reaction of the tridentate aminoalcohol phenol ligands 2,4-di-*tert*-butyl-6-(((2 hydroxyethyl)(methyl)amino)methyl)phenol (**H_2L^1**) and 2,4-di-*tert*-butyl-6-(((1-hydroxybutan-2-yl)amino)methyl)phenol (**H_2L^2**) with $[MoO_2(acac)_2]$ in methanol solutions resulted in the formation of $[MoO_2(\mathbf{L^1})(MeOH)]$ (**1**) and $[MoO_2(\mathbf{L^2})(MeOH)]$ (**3**), respectively. In contrast, the analogous reactions in acetonitrile afforded the dinuclear complexes $[Mo_2O_2(\mu\text{-}O)_2(\mathbf{L^1})_2]$ (**2**) and $[Mo_2O_2(\mu\text{-}O)_2(\mathbf{L^2})_2]$ (**4**). The corresponding reactions with the potentially tetradentate ligand 3-((3,5-di-*tert*-butyl-2-hydroxybenzyl)(methyl)amino)propane-1,2-diol (**H_3L^3**) led to the formation of the mononuclear complex $[MoO_2(\mathbf{L^3})(MeOH)]$ (**5**) in methanol while in acetonitrile solution a trinuclear structure $[Mo_3O_3(\mu\text{-}O)_3(\mathbf{L^3})_3]$ (**6**) was obtained. In both cases, the ligand moiety **L^3** coordinated in a tridentate fashion. The catalytic activities of complexes **1-6** in epoxidation of five different olefins **S1-5** with *tert*-butyl hydroperoxide and hydrogen peroxide were studied. The catalytic activities were found to be moderate to good for the reaction of substrate *cis*-cyclooctene **S1**, while all complexes were less active in the epoxidation of more challenging substrates **S2-5**. The molecular structures of **1**, **2**, **4** and **6** were determined by single crystal X-ray diffraction analyses.

Keywords: Molybdenum complex, Tridentate ligand, Trinuclear structure, Epoxidation

1. Introduction

Complexes containing a *cis*-$[MoO_2]^{2+}$ moiety play crucial roles in catalytic oxidation reactions such as alkene epoxidation [1] and oxotransfer reactions [2,3]. Molybdenum-catalysed epoxidation reactions are of interest for the production of both bulk and fine chemicals [1,4,5]. In a number of studies, dioxidomolybdenum(VI) complexes with chelating phenolate ligands have been used as catalysts for catalytic oxidation reactions such as oxidative bromination, oxotransfer form DMSO to PPh_3 and alkene epoxidation [6].

Aminobisphenol ligands (with two coordinating phenolate moieties in the structure) form a topical group of chelating phenols that can coordinate as tridentate or tripodal tetradentate ligands (if an additional donor group is present) with various transition metals [6a,7,8]. In general, the coordination of tridentate aminomonophenols (containing only one coordinating phenol moiety together with other, e.g. aliphatic alcohol, moieties) to the dioxidomolybdenum(VI) center leaves one vacant coordination site that can be filled either by a solvent molecule or through dimerization [9,10]. The formation of monomeric solvent adducts, dimers and, in some cases, oxido-bridged trinuclear species [11] depends on the experimental conditions. A relatively limited number of aminomonophenolate alcoholate complexes of transition metals [6b,12,17] have been reported in the literature compared with reports on complexes of aminobisphenolate ligands.

In continuation of our research on Mo(VI) and W(VI) complexes with multidentate aminobisphenolate ligands, [6e,13-15] we have investigated the catalytic performance of MoO_2(VI) complexes of several aminoalcohol phenol ligands. In the present study, we have synthesized the three aminomonophenolate ligands containing different aminoalcohols as a side-arm donor moieties, 2,4-di-*tert*-butyl-6-(((2-hydroxyethyl)(methyl)amino)methyl)phenol (**H_2L^1**), 2,4-di-*tert*-butyl-6-(((1-hydroxybutan-2-yl)amino)methyl)phenol (**H_2L^2**) and 3-((3,5-di-tert-butyl-2-hydroxybenzyl)(methyl)amino)propane-1,2-diol (**H_3L^3**) (Figure 1). In ligand **H_3L^3**, the uncoordinated alcoholic hydroxyl group is in close vicinity to the molybdenum centre and may form a hydrogen bond with incoming oxidants like *tert*-butyl hydroperoxide (*t*BuOOH) or hydrogen peroxide (H_2O_2) in the first step of the catalytic epoxidation reaction. The ligand **H_2L^1** was previously used for the preparation of the bis(μ-alkoxido)diiron(III) complexes $[Fe(X_1)\mathbf{L^1}]_2$ (X_1 = $acac^-$, Cl^-) [16] and the monomeric oxidotungsten(VI) complexes $[WO(X_2)(\mathbf{L^1})]$ (X_2 = ethylene glycolate, X = Cl^-) [17]. The magnetic properties of these iron complexes and the ring-opening metathesis polymerization activities of the tungsten complexes were studied. The *L*-isomer of the ligand **H_2L^2** was previously used for *in situ* catalytic asymmetric hydrophosphonylation with Et_2AlCl [18]. To our knowledge, there are no previous publications on ligand (precursor) **H_3L^3**.

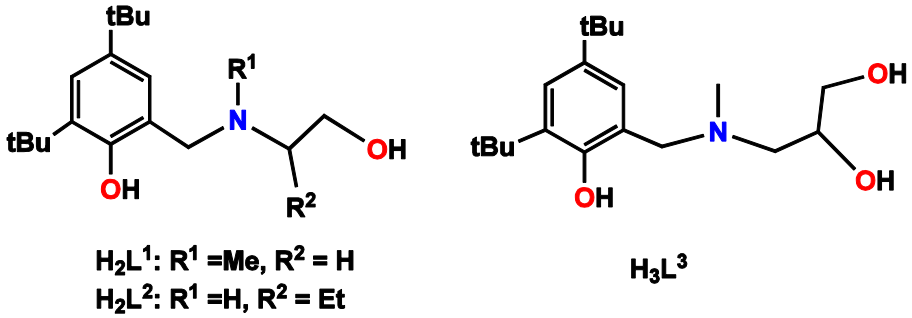

H_2L^1: R^1 =Me, R^2 = H
H_2L^2: R^1 =H, R^2 = Et

H_3L^3

Figure 1. Aminomonophenolate ligands, H_2L^1, H_2L^2 and H_3L^3

In the present investigation, we report the syntheses, characterisations and solid-state structures of new mono- (**1**, **3, 5**), di- (**2**, **4**) and trinuclear (**6**) Mo(VI) complexes with the aforementioned ligands. The catalytic activities of complexes **1-6** in epoxidation of the five olefins *cis*-cyclooctene **S1**, 1-octene **S2**, styrene **S3**, limonene **S4** and α-terpineol **S5** (*vide infra*, Fig. 6) by either hydrogen peroxide or *tert*-butyl hydroperoxide were also investigated.

2. Experimental

2.1. Materials and physical measurements

Commercial grade chemicals were used without further purification and HPLC grade solvents were used as received. All syntheses and manipulations were performed under ambient atmospheric conditions with standard laboratory equipment. NMR spectra were recorded using Bruker Optics 300 MHz or Varian Inova 500 MHz spectrometers with standard settings for ^{1}H and ^{13}C nuclei, using deuterated chloroform and dimethyl sulfoxide as solvents, and referenced to the residual signal of the solvent. Peaks are reported as singlet (s), doublet (d), doublet of doublets (dd), triplet (t) and multiplet (m or unresolved), coupling constants are given in Hz. IR spectra were recorded on a Bruker Vertex 70 spectrometer with wave number (cm^{-1}) and intensities (br = broad, vs = very strong, s = strong, m = medium, w = weak). Mass spectrometry was performed on Waters ZQ 4000 and Waters QTof Xevo-G2 spectrometer using calibrant as CsI. Results are denoted as cationic mass peaks; unit is the mass/charge ratio.

2.2. Preparation of the ligands

H_2L^1 was synthesized by a literature procedure [19].

Preparation of 2,4-di-*tert*-butyl-6-(((1-hydroxybutan-2-yl)amino)methyl)phenol (H_2L^2)

2,4-di-*tert*-butylphenol (4.12 g, 20 mmol), 2-amino-1-butanol (2.74 g, 20 mmol) and paraformaldehyde (0.60 g, 20 mmol) were mixed and heated (110 – 120°C) in a round-bottomed flask for two hours. The reaction mixture was cooled to room temperature and treated with methanol to obtain white crystalline solid. Recrystallization from methanol produced solid product in a 64 % yield (3.90 g). The synthesized aminophenol was characterized by IR and

NMR. Selected IR (cm^{-1}) 2950m (N–H), 1114m (C–N), 766m (N–H wag). ^{1}H NMR (300 MHz, $CDCl_3$) δ 10.21 (s, 1H, Ph-O*H*), 7.25 (d, *J* = 2.4 Hz, 1H, Ar*H*), 6.84 (d, *J* = 2.4 Hz, 1H, Ar*H*), 4.38 (d, *J* = 5.9 Hz, 1H, HNCH_2), 4.31 (d, *J* = 5.9 Hz, 1H, HNCH_2), 4.15 (dt, *J* = 14.2, 7.1 Hz, 1H, HNC*H*), 3.88 (q, *J* = 13.3 Hz, 2H, CH_3CH_2), 3.50-342 (m, 1H, CH_2OH), 3.02 – 2.93 (m, 1H, CH_2OH), 1.73 – 1.59 (m, 1H, CH_2N*H*), 1.43 (s, 9H, C(CH_3)$_3$), 1.30 (s, 9H, C(CH_3)$_3$), 0.94 (t, *J* = 7.4 Hz, 3H, CH_3CH_2). ^{13}C NMR (75 MHz, $CDCl_3$) δ 153.96, 140.82, 136.01, 123.58, 123.32, 121.51 (Ar-C), 84.72 (CH), 69.72 (CH_2), 65.02 (CH_2), 34.88 (CH_2), 34.16 [$C(CH_3)_3$], 31.69 [$C(CH_3)_3$], 29.63 (CH_3), 26.29 (CH_3), 10.77 (CH_3).

Preparation of 3-((3,5-di-*tert*-butyl-2-hydroxybenzyl)(methyl)amino)propane-1,2-diol (H_3L^3)

2,4-di-*tert*-butylphenol (4.12 g, 20 mmol), 3-methylamino-1,2-propanediol (2.74 g, 20 mmol) and paraformaldehyde (0.60 g, 20 mmol) were mixed and heated (110 – 120°C) in a round-bottomed flask for two hours. The reaction mixture was cooled to the room temperature and treated with methanol to obtain white crystalline solid. Recrystallization from methanol produced solid product in a 59 % yield (3.80 g). The synthesized aminophenol was characterized by IR and NMR. Selected FT-IR (cm^{-1}) 2952m (N–H), 1102m (C–N). ^{1}H NMR (500 MHz, DMSO-d_6) δ 7.09 (d, *J* = 2.4 Hz, 1H, Ar*H*), 6.85 (d, *J* = 2.4 Hz, 1H, Ar*H*), 3.72 – 3.68 (m, 1H, OHCH_2C*H*), 3.66 (s, 2H, NCH_2), 3.34 – 3.28 (m, 2H, NCH_3CH_2), 2.51 (dd, *J* = 5.9, 2.9 Hz, 1H, OHCH_2), 2.42 (dd, *J* = 11.0, 5.4 Hz, 1H, OHCH_2), 2.20 (s, 3H, NCH_3), 1.35 (s, 9H, C(CH_3)$_3$), 1.23 (s, 9H, C(CH_3)$_3$). ^{13}C NMR (126 MHz, DMSO-d_6) δ 154.38, 139.85, 134.70, 123.55, 122.14, 122.07 (Ar-C), 69.24 (CH), 65.00 (CH_2), 62.30 (CH_2), 60.44 (CH_2), 41.70 [$C(CH_3)_3$], 34.82 [$C(CH_3)_3$], 34.17 (CH_3), 31.98 (CH_3), 29.91 (CH_3).

*2.3 Preparation of complexes **1**-**6***

[MoO_2(**L^1**)(MeOH)] **1**. [MoO_2(acac)$_2$] 0.130 g (0.40 mmol) and ligand **H_2L^1** 0.117 g (0.40 mmol) were dissolved in 5 mL of methanol. The yellow reaction mixture was stirred at ambient temperature for 2 hours. The resulting yellow solution was allowed to evaporate slowly at room temperature for a few days to obtain yellow crystals suitable for X-ray study. Yield 60% (0.109 g). ^{1}H NMR (500 MHz, DMSO-d_6) δ 7.18 (d, *J* = 2.4 Hz, 1H, Ar*H*), 6.97 (d, *J* = 2.4 Hz, 1H, Ar*H*), 4.66 (td, *J* = 11.8, 3.2 Hz, 1H, NCH_2), 4.48 (dd, *J* = 11.0, 5.4 Hz, 1H, NCH_2CH_2), 4.21 (d, *J* = 12.2 Hz, 1H, NCH_2), 4.10 (q, *J* = 5.2 Hz, CH_3O*H*), 3.27 – 3.23 (m, 2H, CH_3NCH_2), 3.17 (d, *J* = 4.9 Hz, CH_3OH), 2.65 (dd, *J* = 11.5, 3.0 Hz, 1H, NCH_2CH_2), 2.46 (s, 3H, NCH_3), 1.35 (s, 9H, C(CH_3)$_3$), 1.25 (s, 9H, C(CH_3)$_3$). ^{13}C NMR (75 MHz, DMSO-d_6) δ 158.70, 141.12, 136.82, 125.12, 123.86, 123.22 (Ar-C), 71.77 (CH_2), 62.12 (CH_2), 61.52 (CH_2), 49.06 (CH_3), 44.67 [$C(CH_3)_3$], 35.20 [$C(CH_3)_3$], 34.31 (CH_3), 31.97 (CH_3), 30.54 (CH_3). Selected IR resonances (cm^{-1}) 3087 (O-H, MeOH) 929s (Mo=O), 901s (Mo=O). ESI-MS: *m/z* = 487 [**1**·MeOH+H]$^+$, 444 [**1**-MeOH+Na]$^+$, 294 [**H_2L^1**+H]$^+$.

[Mo_2O_2(μ-O)$_2$(**L^1**)$_2$] **2**. [MoO_2(acac)$_2$] 0.130 g (0.40 mmol) and ligand **H_2L^1** 0.117 g (0.40 mmol) were dissolved in 5 mL of anhydrous acetonitrile. The orange reaction mixture was stirred at ambient temperature for 4 hours. The resulting orange solution was left to evaporate slowly at room temperature to obtain orange crystals suitable for X-ray study. Yield

65% (0.218 g). ^{1}H NMR (500 MHz, DMSO-d$_6$) δ 7.18 (d, *J* = 2.4 Hz, 2H, Ar*H*), 6.98 (d, *J* = 2.4 Hz, 2H, Ar*H*), 4.66 (td, *J* = 11.8, 3.2 Hz, 2H, NC*H*$_2$), 4.47 (dd, *J* = 11.0, 5.4 Hz, 2H, NCH$_2$C*H*$_2$), 4.20 (d, *J* = 12.2 Hz, 2H, NC*H*$_2$), 3.27 – 3.24 (m, 4H, CH$_3$NC*H*$_2$), 2.65 (dd, *J* = 11.0, 5.4 Hz, 2H, NCH$_2$C*H*$_2$), 2.46 (s, 6H, NC*H*$_3$), 1.35 (s, 18H, C(C*H*$_3$)$_3$), 1.25 (s, 18H, C(C*H*$_3$)$_3$). ^{13}C NMR (126 MHz, CDCl$_3$) δ 157.97, 142.84, 137.54, 124.13, 123.47, 122.01(Ar-C), 72.97 (CH$_2$), 63.17 (CH$_2$), 62.87 (CH$_2$), 45.25 [C(CH$_3$)$_3$], 35.14 [C(CH$_3$)$_3$], 34.29 (CH$_3$), 31.64 [C(CH$_3$)$_3$], 30.31 [C(CH$_3$)$_3$]. Selected IR resonances (cm^{-1}) 913m (Mo=O), 877s (Mo–O–Mo), 842m (Mo–O–Mo). ESI-MS: *m/z* = 863 [**2**+Na]$^+$, 841 [**2**+H]$^+$, 294 [**H$_2$L^1**+H]$^+$.

[MoO$_2$(**L^2**)(MeOH)] **3**. [MoO$_2$(acac)$_2$] 0.130 g (0.40 mmol) and ligand **H$_2$L^2** 0.123 g (0.40 mmol) were dissolved in 5 mL of methanol. The yellow reaction mixture was stirred at room temperature with magnetic stirring for 2 hours. Subsequently the resulting yellow solution was allowed to stand at room temperature for slow evaporation to grow yellow microcrystals. Yield 55% (0.102 g). ^{1}H NMR (500 MHz, DMSO-d$_6$) δ 7.14 (d, *J* = 2.4 Hz, 1H, Ar*H*), 7.02 (d, *J* = 2.4 Hz, 1H, Ar*H*), 5.07 (td, *J* = 11.0, 2.9 Hz, 1H, NC*H*$_2$), 4.63 (dd, *J* = 11.0, 5.4 Hz, 1H, NC*H*$_2$), 4.10 (q, *J* = 5.2 Hz, CH$_3$O*H*), 3.97 (t, *J* = 10.6 Hz, 1H, NHC*H*), 3.78 – 3.68 (m, 2H, OC*H*$_2$), 3.17 (d, *J* = 4.9 Hz, C*H*$_3$OH), 2.92 – 2.86 (m, 1H, CH$_3$C*H*$_2$), 1.48 – 1.41 (m, 1H, CH$_3$C*H*$_2$), 1.35 (s, 9H, C(C*H*$_3$)$_3$), 1.25 (s, 9H, C(C*H*$_3$)$_3$), 0.89 (t, *J* = 7.6 Hz, 3H, C*H*$_3$CH$_2$). ^{13}C NMR (126 MHz, DMSO-d$_6$) δ 159.36, 140.56, 136.76, 125.70, 124.75, 122.86 (Ar-C), 78.52 (CH), 63.88 (CH$_2$), 48.86 (CH$_2$), 35.16 (CH$_2$), 34.29 [C(CH$_3$)$_3$], 31.98 [C(CH$_3$)$_3$], 30.63 (CH$_3$), 21.42 (CH$_3$), 11.67(CH$_3$). Selected IR resonances (cm^{-1}) 3196 (O-H, MeOH) 953m (Mo=O), 920s (Mo=O). ESI-MS: *m/z* = 521 [**3**·MeOH+Na]$^+$, 499 [**3**.MeOH+H]$^+$, 458 [**3**-MeOH+Na]$^+$, 308 [**H$_2$L^2**+H]$^+$.

[Mo$_2$O$_2$(*μ*-O)$_2$(**L^2**)$_2$] **4**. [MoO$_2$(acac)$_2$] 0.130 g (0.40 mmol) and ligand **H$_2$L^2** 0.123 g (0.40 mmol) were dissolved in 5 mL of anhydrous acetonitrile. The orange reaction mixture was stirred at ambient temperature for 4 hours. X-ray quality orange crystals were obtained by slow evaporation of the resulting solution at room temperature. Yield 75% (0.260 g). ^{1}H NMR (500 MHz, DMSO-d$_6$) δ 7.15 (d, *J* = 2.4 Hz, 2H, Ar*H*), 7.02 (d, *J* = 2.4 Hz, 2H, Ar*H*), 5.06 (td, *J* = 11.0, 2.9 Hz, 2H, NC*H*$_2$), 4.63 (dd, *J* = 11.0, 5.4 Hz, 2H, NC*H*$_2$), 3.97 (t, *J* = 10.6 Hz, 2H, NHC*H*), 3.78 – 3.68 (m, 4H, OC*H*$_2$), 2.93 – 2.86 (m, 2H, CH$_3$C*H*$_2$), 1.50 – 1.40 (m, 2H, CH$_3$C*H*$_2$), 1.35 (s, 18H, C(C*H*$_3$)$_3$), 1.25 (s, 18H, C(C*H*$_3$)$_3$), 0.89 (t, *J* = 7.6 Hz, 6H, C*H*$_3$CH$_2$). ^{13}C NMR (75 MHz, DMSO-d$_6$) δ 159.39, 140.58, 136.76, 125.73, 124.78, 122.88 (Ar-C), 78.54 (CH), 63.88 (CH$_2$), 48.86 (CH$_2$), 40.76 (CH$_2$), 35.18 [C(CH$_3$)$_3$], 34.31 [C(CH$_3$)$_3$], 32.00 (CH$_3$), 30.64 (CH$_3$), 21.44 (CH$_3$). Selected IR resonances (cm^{-1}) 919m (Mo=O), 868s (Mo–O–Mo), 818m (Mo–O–Mo). ESI-MS: *m/z* = 890 [**4**+Na]$^+$, 867 [**4**+H]$^+$, 308 [**H$_2$L^2**+H]$^+$.

[MoO$_2$(**L^3**)(MeOH)] **5**. [MoO$_2$(acac)$_2$] 0.163 g (0.50 mmol) and ligand **H$_3$L^3** 0.162 g (0.50 mmol) were dissolved in 5 mL of methanol. The yellow reaction mixture was stirred at ambient temperature for 2 hours. The resulting yellow solution was then left to evaporate slowly at room temperature to afford yellow microcrystals of the complex. Yield 55% (0.137 g). ^{1}H NMR (500 MHz, DMSO-d$_6$) δ 7.18 (d, *J* = 2.4 Hz, 1H, Ar*H*), 6.97 (d, *J* = 2.4 Hz, 1H, Ar*H*), 4.80 – 4.78 (m, 2H, NC*H*$_2$), 4.20 (d, *J* = 12.2 Hz, 1H, OHC*H*$_2$), 4.10 (q, *J* = 5.2 Hz, CH$_3$O*H*), 3.50 – 3.42 (m, 2H, NCH$_3$C*H*$_2$), 3.23 (d, *J* = 12.2 Hz, 1H, OHC*H*$_2$), 3.17 (d, *J* = 4.9

Hz, CH_3OH), 3.07 (t, *J* = 11.3 Hz, 1H, $OHCH_2$), 2.73 (dd, *J* = 11.4, 3.3 Hz, 1H, $OHCH_2CH$), 2.50 (s, 3H, NCH_3), 1.35 (s, 9H, $C(CH_3)_3$), 1.25 (s, 9H, $C(CH_3)_3$). ^{13}C NMR (126 MHz, DMSO-d_6) δ 158.64, 141.10, 136.75, 125.09, 123.95, 123.20 (Ar-C), 82.97 (CH), 64.43 (CH_2), 63.71 (CH_2), 62.06 (CH_2), 45.62 (CH_3), 35.17 [$C(CH_3)_3$], 34.29 [$C(CH_3)_3$], 31.95 (CH_3), 30.50 (CH_3). Selected IR resonances (cm^{-1}) 3395 (O-H, MeOH) 934s (Mo=O), 915s (Mo=O). ESI-MS: *m/z* = 506 [**5**+Na]$^+$, 474 [**5**-MeOH+Na]$^+$, 452 [**5**-MeOH+H]$^+$, 324 [$\mathbf{H_3L^3}$+H]$^+$.

[{MoO_2($\mathbf{L^3}$)}$_3$] 6. [$MoO_2(acac)_2$] 0.163 g (0.50 mmol) and ligand $\mathbf{H_3L^3}$ 0.162 g (0.50 mmol) were dissolved in 5 mL of anhydrous acetonitrile. The orange reaction mixture was stirred at ambient temperature for 4 hours. The resulting orange solution was allowed to evaporate slowly at room temperature to obtain crystalline material. Recrystallization from hot chloroform solution yielded single crystal suitable for X-ray analysis. Yield 50% (0.396 g). ^{1}H NMR (500 MHz, DMSO-d_6) δ 7.18 (d, *J* = 2.4 Hz, 3H, Ar*H*), 6.97 (d, *J* = 2.4 Hz, 3H, Ar*H*), 4.79 – 4.77 (m, 6H, NCH_2), 4.19 (d, *J* = 12.2 Hz, 3H, $OHCH_2$), 3.51 – 3.42 (m, 6H, NCH_3CH_2), 3.22 (d, *J* = 12.2 Hz, 3H, $OHCH_2$), 3.07 (t, *J* = 11.3 Hz, 3H, $OHCH_2$), 2.74 (dd, *J* = 11.4, 3.3 Hz, 3H, $OHCH_2CH$), 2.50 (s, 9H, NCH_3), 1.35 (s, 27H, $C(CH_3)_3$), 1.25 (s, 27H, $C(CH_3)_3$). ^{13}C NMR (126 MHz, DMSO-d_6) δ 158.64, 141.10, 136.75, 125.09, 123.95, 123.21 (Ar-C), 82.94 (CH), 64.43 (CH_2), 63.72 (CH_2), 62.06 (CH_2), 45.63 (CH_3), 35.17 [$C(CH_3)_3$], 34.29 [$C(CH_3)_3$], 31.95 (CH_3), 30.50 (CH_3). Selected IR resonances (cm^{-1}) 3410 (O-H, alcoholic OH), 967s (Mo=O), 928s (Mo=O), 912s (Mo=O), 856s (Mo–O–Mo), 836s (Mo–O–Mo). ESI-MS: *m/z* = 1371 [Mo_3O_6($\mathbf{L^3}$)$_3$+Na]$^+$, 923 [Mo_2O_4($\mathbf{L^3}$)$_2$+Na]$^+$, 474 [MoO_2($\mathbf{L^3}$)+Na]$^+$, 324 [$\mathbf{H_3L^3}$+H]$^+$.

2.4. Catalysis studies

2.4.1. Epoxidation

Experiments were carried out in a Heidolph Parallel Synthesizer 1. In a typical experiment, 2−3 mg of catalyst (1 mol%) was dissolved in 0.5 mL of $CHCl_3$ and mixed with 1 equiv. of substrate. Then 50 µL of mesitylene were added as internal standard, and the reaction mixtures were heated to 50 °C, whereupon the oxidant (3 equiv.) was added in one portion. Aliquots for GC−MS (20 µL) were withdrawn with a calibrated Socorex Acura 825, 10−100 µL variable volume pipet at given time intervals, quenched with MnO_2, and diluted with HPLC-grade ethyl acetate. The reaction products were analyzed by GC−MS (Agilent Technologies 7890 GC System), and the epoxide produced from each reaction mixture was quantified versus mesitylene as the internal standard.

2.5. X-ray structure determination

The crystals of **1**, **2**, **4** and **6** were immersed in cryo-oil, mounted in a MiTeGen loop, and measured at a temperature of 120 K on a Bruker Kappa Apex II or on a Rigaku Oxford Diffraction Supernova diffractometer using Mo Kα (λ = 0.71073) radiation. The *CrysAlisPro* [20] or *Denzo-Scalepack* [21] program packages were used for cell refinements and data reductions. Multi-scan absorption corrections (*SADABS* [22] or *CrysAlisPro* [20]) were applied to the intensities before structure solutions. The structures were solved by charge flipping

method using the *SUPERFLIP* [23] software or by using direct methods and *SHELXT* [24] program. Structural refinements were carried out using *SHELXL* [24]. In **1** the coordinates of the OH hydrogen atom were refined on a riding model (fixed distance) with U_{iso} = 1.5·U_{eq} parent oxygen. All other H-atoms were positioned geometrically and constrained to ride on their parent atoms, with C-H = 0.95-1.00 Å, O-H = 0.84 Å and U_{iso} = 1.2-1.5·U_{eq} (parent atom).

3. Results and discussion

3.1. Syntheses and spectroscopic characterization of complexes

All ligands were prepared by Mannich reactions, applying a solvent-free procedure consisting of mixing stoichiometric amounts of 2,4-di-*tert*-butylphenol, paraformaldehyde and the appropriate aminoalcohol, and heating the reaction mixture in an open vessel. The mononuclear complexes [MoO_2(**L^1**)(MeOH)] (**1**) and [MoO_2(**L^2**)(MeOH)] (**3**) were prepared by the treatment of [$MoO_2(acac)_2$] with one equivalent of ligand in methanol at ambient temperature. The analogous reactions in acetonitrile solutions led to the formation of the dinuclear complexes [$Mo_2O_2(\mu\text{-}O)_2$(**L^1**)$_2$] (**2**) and [$Mo_2O_2(\mu\text{-}O)_2$(**L^2**)$_2$] (**4**) (Scheme 1). The complexes crystallised from the reaction mixtures upon slow evaporation of the solvents. Complexes **1** and **3** are soluble in polar solvents such as acetonitrile, tetrahydrofuran, chloroform, dichloromethane, while the dinuclear complexes **2** and **4** may be dissolved in hot MeOH and DMSO but are practically insoluble in any other solvents.

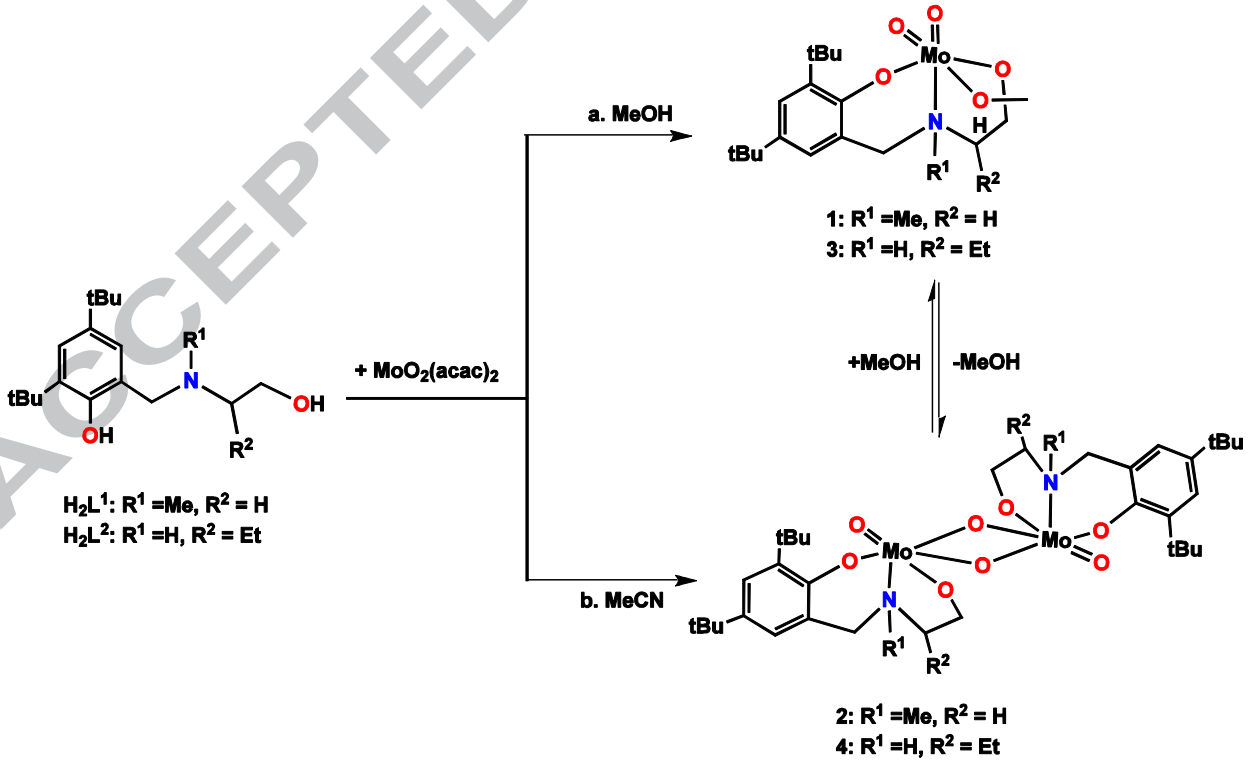

Scheme 1. Formation of mononuclear and dinuclear Mo(VI) complexes with ligands **H_2L^1** and **H_2L^2**.

The coordinated MeOH in **1** and **3** evaporates slowly in open air and more rapidly in vacuum to yield the dinuclear complexes **2** and **4**, respectively. Similarly, when dissolved in acetonitrile, the monomeric complexes are converted into their analogous dimers and precipitate from the solutions as orange powders. Conversely, complexes **1** and **3** can be obtained from complexes **2** and **4** by dissolution in hot MeOH solvent.

The ligand $\mathbf{H_3L^3}$ reacts with $[MoO_2(acac)_2]$ in methanol to form the monomeric complex $[MoO_2(\mathbf{L^3})(MeOH)]$ (**5**) with a dangling OH group as yellow crystals (Scheme 2). Based on the observations discussed above, the analogous reaction in acetonitrile was expected to lead to the formation of a dimeric complex. However, single crystal X-ray diffraction (*vide infra*) showed that $[Mo_3O_3(\mu\text{-}O)_3(\mathbf{L^3})_3]$ (**6**) is a trinuclear complex where the molybdenum and oxygen atoms form a planar six-membered Mo_3O_3 ring (Scheme 2). When a methanol solution of **6** was concentrated by slow evaporation at room temperature, the yellow solid that precipitated was characterised by IR to be identical with mononuclear complex **5**.

In conclusion, the formation of monomeric and dimeric complexes based on the ligands in this study may be controlled by the choice of solvent. Specifically, the monomeric complexes can be transformed to their dimeric counterparts by removal of the coordinated methanol ligand, while dimers may be converted into monomers by dissolution in MeOH. Previous work with oxidomolybdenum(VI) complexes with tri- and tetradentate aminobisphenols as well as Schiff base ligands has shown similar reactivity [6h,10,25].

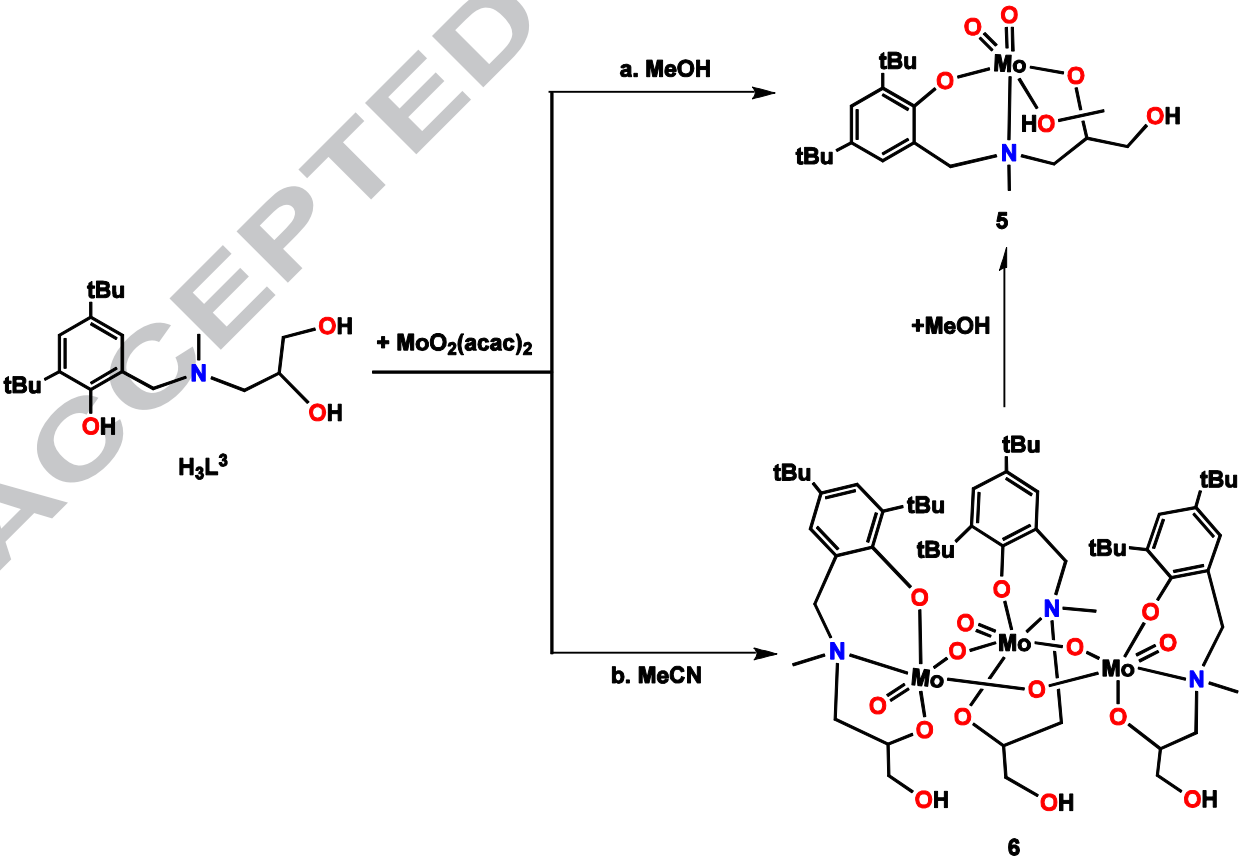

Scheme 2. Formation of mononuclear and trinuclear Mo(VI) complexes with ligand $\mathbf{H_3L^3}$

The IR spectra for the mononuclear MoO_2(VI) complexes (**1**, **3** and **5**) exhibit two strong $\nu_{Mo=O}$ bands around 901-920 and 929-953 cm^{-1} corresponding to the antisymmetric and symmetric stretching modes, respectively, for the *cis*-$[MoO_2]^{2+}$ moiety [26-28]. Broad bands at ~ 3087-3395 cm^{-1} are characteristic for coordinated or hydrogen bonded methanol molecules. The μ-oxido-bridged dinuclear MoO(VI) complexes **2** and **4** show only a single vibrational band at 913 and 919 cm^{-1}, respectively, in their spectra instead of the characteristic doublets for *cis*-$[MoO_2]^{2+}$ fragments. In addition, **2** and **4** display strong absorptions in the 877-818 cm^{-1} range that are diagnostic for Mo=O···Mo bridges due to the weakened Mo=O bond [10]. The trinuclear complex **6** showed three characteristic bands at 912, 928 and 967 cm^{-1} for $\nu_{Mo=O}$ and the antisymmetric oxygen bridges present strong bands at 836 and 856 cm^{-1}.

The ^1H and ^{13}C NMR spectra in deuterated dimethyl sulfoxide solution showed the expected resonances for aminophenolate alcoholate ligands. For all complexes, disappearance of the phenolate OH signals in the ^1H NMR spectra of the aminophenolate alcoholate ligands confirm the deprotonation of the ligands upon complexation. The NMR spectra of all complexes showed the expected resonances for the tridentate ligands. Complexes **1**, **3** and **5** showed similar chemical shifts (as well as the resonances for free MeOH) as their dimeric or trimeric counterparts, which indicates, that the complexes adopt comparable solution structures, possibly due to the coordination of DMSO and formation of monomeric species; such dissociation of the trimeric molybdenum-oxo species [{MoO_2(L)}$_3$] (H_2L = 2,4-di-*tert*-butyl-6-(((2-hydroxy-2-phenylethyl)amino)methyl)phenol), related to **6**, has been demonstrated previously [29].

In the ^1H NMR spectra of complexes **1** and **2**, the diastereotopic benzylic CH_2-protons exhibit two separate signals. One signal is seen at 4.66 ppm as a doublet of triplet (td, J = 11.8, 3.2 Hz) due to the long-range coupling to the N-CH_2 protons as well as to the geminal proton, and the second proton shows up as a doublet (d, J = 12.2 Hz) at *ca.* 4.20 ppm due to the geminal coupling of a benzylic proton. The N-Me protons resonate at 2.46 ppm. Similarly, for complexes **3** and **4**, the benzylic protons show a doublet of triplet at 5.07 ppm with coupling constants J = 11.0, 2.9 Hz for one proton while the other proton is seen at 4.63 ppm as a doublet of doublets with coupling constants J = 11.0, 5.4 Hz. For complexes **5** and **6**, the benzylic protons are seen as a broad multiplet at *ca*. 4.78 ppm. For complexes **1**, **3** and **5**, the coordinated methanol OH proton appears as a quartet at 4.10 ppm while the methyl protons are seen as a doublet at 3.17 ppm. For **3** and **4**, some uncharacterised minor peaks were seen in the spectra, possibly due to slow decomposition in solution.

The metal complexes were characterized by mass spectrometry using electrospray ionisation. In all mass spectra of the mono-, di- and trinuclear complexes there are ions of significant intensity that can be attributed to the dissociated aminophenolate ligands. The spectra of complexes **1**, **3** and **5** contained the molecular peaks at *m/z* = 487, 521 and 506 because of the ions [**1**·MeOH+H]$^+$, [**3**·MeOH+Na]$^+$and [**5**+Na]$^+$, respectively.

The dinuclear complexes **2** and **4** showed prominent peaks at *m/z* = 863 *m/z* = 890 corresponding to the species [**2**+Na]$^+$ and [**4**+Na]$^+$ as well as peaks for mononuclear species.

Similarly, the trinuclear **6** complex displayed a major molecular peak for $[\mathbf{6}+Na]^+$, (*m/z* = 1371) and characteristic peaks for dimeric and monomeric structures. All complexes containing metal ions displayed the predicted isotopic distributions with relative intensities and *m/z* values that are consistent with the most abundant isotopic composition.

3.2. Crystal and molecular structures

The molecular structures of complexes **1**, **2**, **4** and **6**·2$CHCl_3$ were determined by single-crystal X-ray diffraction analyses. Their molecular structures are shown in Figures 2-5. A summary of the crystallographic data and final refinement details are given in Table 1. Selected bond lengths and angles relevant to the coordination spheres of the molybdenum atoms are listed in Table 2. The single crystals of complexes **1**, **2** and **4** were isolated directly from the reaction mixtures. Crystals of **6** isolated from acetonitrile were of rather low quality, but single crystals suitable for X-ray analysis could be grown from chloroform, and two molecules of chloroform were found in the asymmetric unit.

Table 1. Crystallographic data for compounds **1**, **2**, **4** and **6**.

	1	**2**	**4**	**6**
empirical formula	$C_{19}H_{33}MoNO_5$	$C_{36}H_{58}Mo_2N_2O_8$	$C_{38}H_{62}Mo_2N_2O_8$	$C_{59}H_{95}Cl_6Mo_3N_3O_{15}$
fw	451.40	838.72	866.77	1586.89
temp (K)	120(2)	120(2)	120(2)	120(2)
λ(Å)	0.71073	0.71073	0.71073	0.71073
cryst syst	Monoclinic	Monoclinic	Monoclinic	Triclinic
space group	$P2_1/c$	$P2_1/c$	$P2_1/n$	$P\bar{1}$
a (Å)	12.5882(2)	17.0417(3)	a = 8.6913(2)	16.1436(8)
b (Å)	11.9673(2)	9.33570(10)	b = 12.7016(3)	16.4390(8)
c (Å)	14.3727(3)	12.3744(2)	c = 18.4454(3)	16.8147(8)
α (°)	90	90	90	78.792(4)
β (°)	106.1860(10)	102.1160(10)	92.7890(10)	62.009(5)
γ (°)	90	90	90	70.992(5)
V (Å^3)	2079.38(7)	1924.87(5)	2033.84(7)	3720.9(4)
Z	4	2	2	2
ρ_{calc} (Mg/m^3)	1.442	1.447	1.415	1.416
μ(Kα) (mm^{-1})	0.658	0.701	0.666	0.771
No. reflns.	31955	28428	33774	27872
Unique reflns.	6078	4969	5943	17489
GOOF (F^2)	1.107	1.103	1.086	1.045
R_{int}	0.0414	0.0432	0.0392	0.0446
R1[a] ($I \geq 2\sigma$)	0.0311	0.0338	0.0314	0.0666
wR2[b] ($I \geq 2\sigma$)	0.0787	0.0645	0.0637	0.1468

[a] $R1 = \Sigma||F_o| - |F_c||/\Sigma|F_o|$. [b] $wR2 = [\Sigma[w(F_o^2 - F_c^2)^2]/\Sigma[w(F_o^2)^2]]^{1/2}$.

Table 2. Selected bond lengths [Å] and angles [°] for complexes **1**, **2**, **4** and **6**

[Å, °]	**1**	**2**	**4**	**6**
Mo(1)-O(1)	1.9363(12)	1.9212(15)	1.9321(13)	1.899(3)
Mo(1)-O(2)	1.9666(11)	1.9050(16)	1.9023(13)	1.935(4)
Mo(1)-O(3)	1.7132(12)	1.6904(17)	1.7076(14)	1.695(4)
Mo(1)-O(4)	1.6974(13)	1.7559(16)	1.7528(13)	1.751(4)
Mo(1)-O(5)	2.3935(12)	2.4068(16)[a]	2.3688(13)[a]	2.287(4)[d]
Mo(1)-N(1)	2.3745(13)	2.3717(19)	2.3010(15)	2.354(4)
O(1)-Mo(1)-O(2)	149.56(5)	150.28(7)	151.89(6)	151.54(16)
O(4)-Mo(1)-O(3)	105.53(6)	106.80(8)	108.92(6)	104.55(19)
O(3)-Mo(1)-N(1)	161.49(5)	158.03(7)	155.84(6)	163.88(17)
O(4)-Mo(1)-O(5)	170.75(5)	176.30(7)[b]	172.43(6)[b]	168.59(16)
N(1)-Mo(1)-O(5)	78.71(4)	82.04(6)[c]	78.97(5)[c]	77.75(15)
C(1)-O(1)-Mo(1)	136.72(10)	136.33(14)	128.99(11)	140.3(3)
C(19)-O(5)-Mo(1)	119.01(10)			

[a] A parameter for a Mo(1)-O(4)^{i} where i = -*x*, -*y*+1, -*z*+1.
[b] O(3)-Mo(1)-O(4)^{i}.
[c] N(1)-Mo(1)-O(4)^{i}.
[d] A parameter for a Mo(1)-O(3)^{i} where i = -*x*, -*y*, -*z*.

The molecular structures of all complexes reveal hexacoordinate metal centres in distorted octahedral geometries. In complex **1**, the fully deprotonated ligand $(\mathbf{L^1})^{2-}$ is coordinated to the *cis*-dioxidomolybdenum centre in a tridentate coordination mode through its alkoxido oxygen, amine nitrogen and phenolate oxygen atoms. The remaining coordination site *trans* to one oxido ligand is occupied by the oxygen of a coordinated methanol molecule. The Mo-$O_{solvent}$ bond *trans* to the oxido group is considerably longer than the Mo–$O_{phenolate}$ bond due to the strong *trans* influence of the oxido group. These features as well as the O=Mo=O angles and the Mo=O bonds are similar to those found for other mononuclear *cis*-$[MoO_2]^{2+}$ complexes [9,30-33]. The coordinated MeOH molecule from the adjacent unit forms a hydrogen bond to the oxido ligand O(2), with the observed O(5)-H(5) ···O(2)^{i} (i = -x+1, -y+1, -z+1) distance of 2.6976(16) Å being indicative of rather strong intermolecular hydrogen bonding in the solid state. The overall structure of **1** can be compared with those obtained for mononuclear dioxidomolybdenum(VI) complexes $[MoO_2(L)(ROH)]$, where L = aroylhydrazone Schiff base ligand or ephedrine derivative ligand, R = Et or Me [11,34-36].

In the solid state, complexes **2** and **4** have a dinuclear structure, which consists of doubly bridged units of $[Mo_2O_2(\mu\text{-}O)_2(O_{phenolate},N_{amine},O_{alcoholate})_2]$. Each molybdenum(VI) ion is bonded to three donor atoms $O_{phenolate},N_{amine},O_{alcoholate}$ of the tridentate ligands, two bridging oxygen atoms and one terminal oxido ligand to yield a distorted octahedral coordination sphere. Both complexes have a centrosymmetric structure with identical conformations. The Mo(VI) ions with asymmetric di-μ-oxido-bridges form four-membered Mo–O–Mo–O rings, the Mo–O distances being (1.7559(16) and 2.4068(16)) Å for **2** and (1.7528(13) and 2.3688(13)) Å for **4**. The long Mo···O distances indicate a rather weak coordination, which is seen in the reactivity of the complexes. All Mo=O and Mo···O distances are rather similar to those observed for the closely related dinuclear dioxidomolybdenum(VI) complexes $[MoO_2(L)]_2$, where H_2L = an

aroylhydrazone ligand, an (R)-1,1'-binaphthyl-based dioxidoanionic pyridine ligand or a tridentate Schiff base ligands [33,37-39]. In general, there are rather small differences between the structural parameters around the Mo centre in monomeric **1** compared with the dimeric **2** and **4** (see Table 2).

The solid state structure of **6** consists of a trinuclear core where the molybdenum and oxygen atoms form a planar six-membered Mo_3O_3 ring (Figure 5), so the complex unit in **6** has a formal 3-fold axis. Each Mo(VI) ion is bonded to three donor atoms of the organic ligand as well as two bridging and one terminal oxido ligand, resulting in a distorted octahedral coordination sphere. One alcohol OH donor group of the ligand is not participating in the coordination to the metal centre. The oxygen bridges are asymmetric, *e.g.* the Mo1-O1 distance is 1.695(4) Å whereas the Mo1-O3 distance is 2.287(4) Å, which indicates a rather weak intramolecular association of the monomeric species through a Mo=O→Mo coordination and the Mo=O···Mo bridges are unsymmetrical in the dimeric and trimeric Mo complexes. The terminal oxido groups are located in the Mo_3O_3 plane and the tridentate ligand is bonded to the Mo(VI) centres in a meridional coordination mode, vertical to the Mo_3O_3 plane. The trimeric structure is stabilized by three intramolecular H-bonds between the OH groups of the alcohol side-arms and the alkoxide oxygen atoms of the adjacent Mo-centred units with O···O distances of 2.747(5)-2.769(5) Å. The overall structure is closely related to [{MoO_2(L)}$_3$] (H_2L = 2,4-di-*tert*-butyl-6-(((2-hydroxy-2-phenylethyl)amino)methyl)phenol) reported previously by us [29]. Typically, the dioxidomolybdenum(VI) complexes with ONO-type tridentate ligands seem to complete the octahedral coordination sphere by a coordinating solvent molecule, if present, or by oxido ligand from the adjacent molybdenum complex unit to form a dinuclear oxo-bridged complex [10,40].

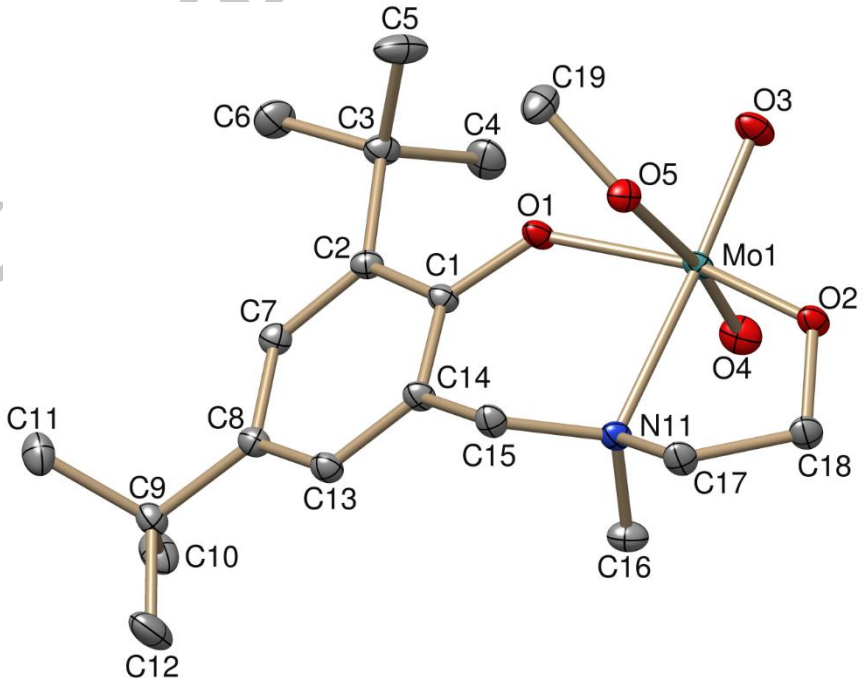

Figure 2. The molecular structure of [MoO_2(**L**^{1})(MeOH)] (**1**). Hydrogen atoms are omitted for the sake of clarity. Thermal ellipsoids are drawn at the 50% probability level.

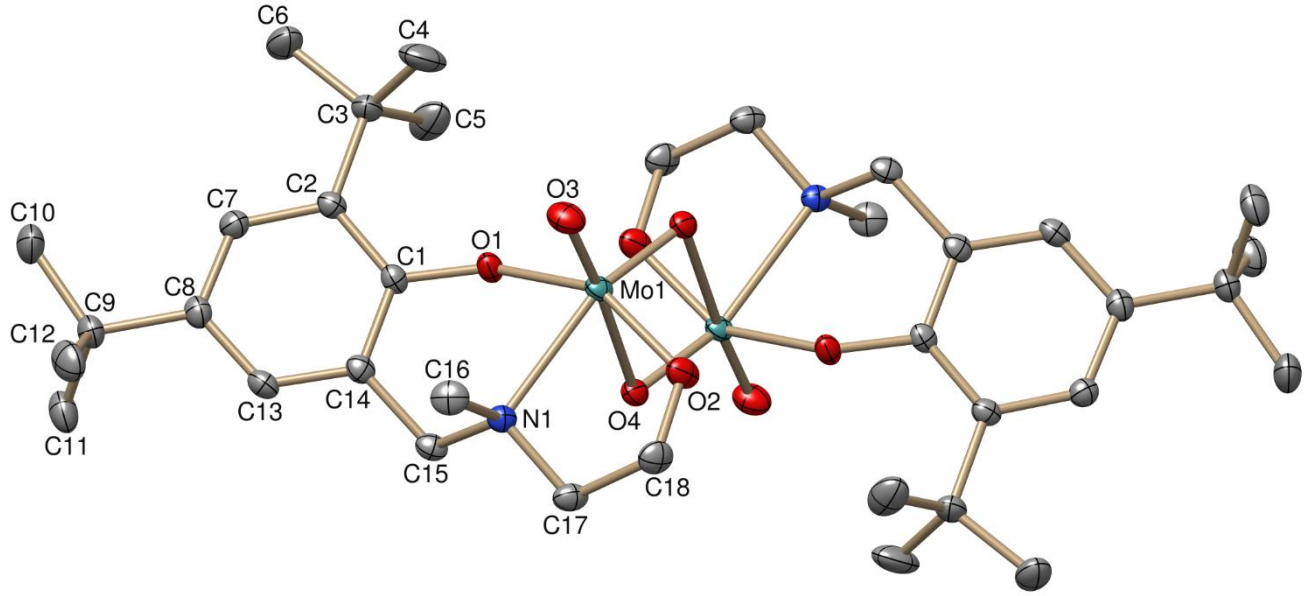

Figure 3. The molecular structure of $[Mo_2O_2(\mu\text{-}O)_2(\mathbf{L}^1)_2]$ (**2**). Hydrogen atoms are omitted for the sake of clarity. Thermal ellipsoids are drawn at the 50% probability level.

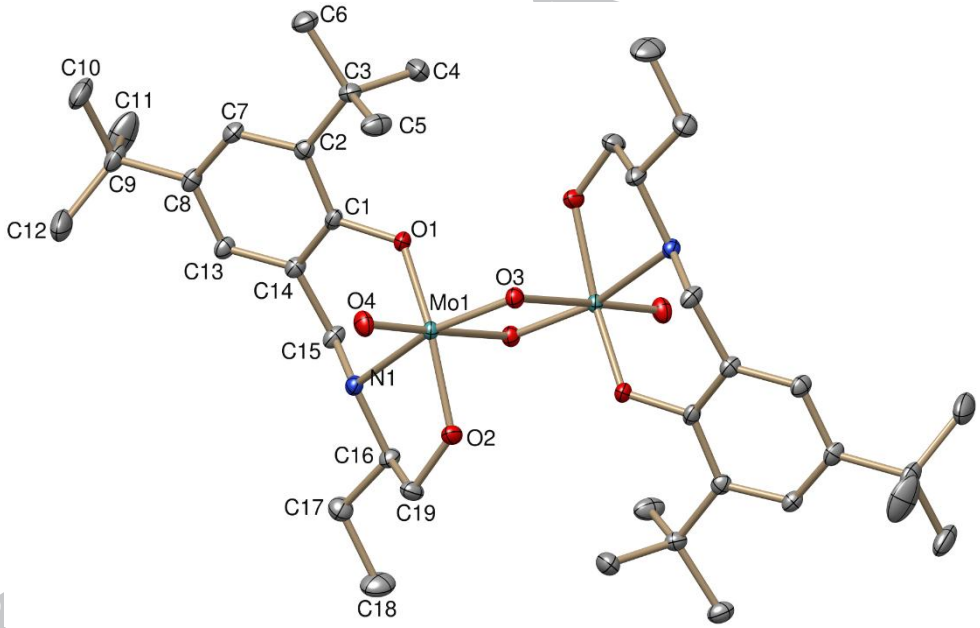

Figure 4. The molecular structure of $[Mo_2O_2(\mu\text{-}O)_2(\mathbf{L}^2)_2]$ (**4**). Hydrogen atoms are omitted for the sake of clarity. Thermal ellipsoids are drawn at the 50% probability level.

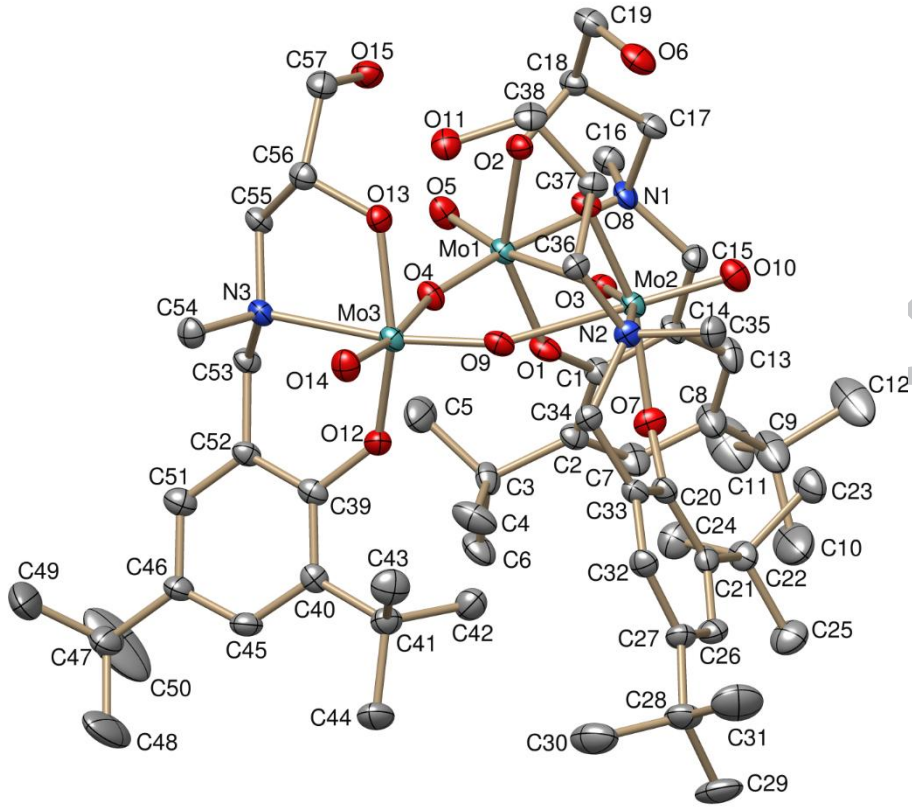

Figure 5. The molecular structure of $[Mo_3O_3(\mu\text{-}O)_3(\mathbf{L^3})_3]$ (**6**). Hydrogen atoms and solvent molecules are omitted for the sake of clarity. Thermal ellipsoids are drawn at the 50% probability level.

3.3. Catalytic epoxidation

Complexes **1**-**6** were tested as catalysts for epoxidation of the five olefinic substrates *cis*-cyclooctene **S1**, 1-octene **S2**, styrene **S3**, limonene **S4** and α-terpineol **S5** (Figure 6), using three equivalents of *tert*-butyl hydroperoxide (TBHP, 5.5 M in decane) or aqueous hydrogen peroxide (H_2O_2, 30%) as oxidants and 1 mol% catalyst loadings. The reactions were run at 50 °C in $CHCl_3$ solutions and conversions to epoxides were followed by GC–MS. In the case of substrates **S4** and **S5**, racemic mixtures of the *D*- and *L*-enantiomers were used. The results are shown in Table 3.

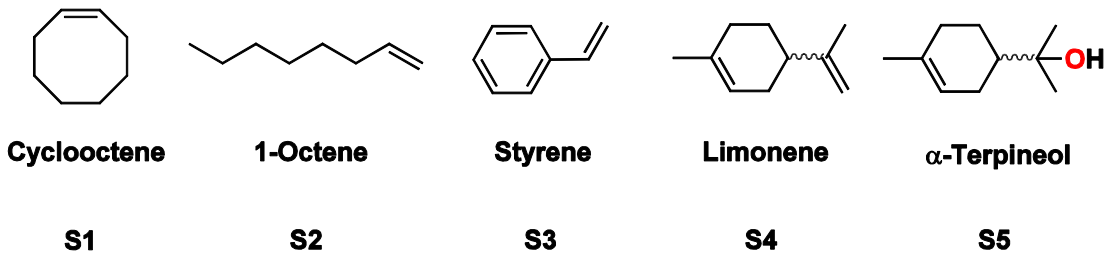

Figure 6. Olefinic substrates used for epoxidation experiments.

With TBHP as oxidant, all six Mo complexes convert **S1** quantitatively to its epoxide with excellent selectivities within 24 h, reaching yields of >95% epoxide. Interestingly, there was no significant difference in activity observed for monomeric complexes **1** and **3** with respect to their dimeric counterparts **2** and **4**. These four complexes also did not differ significantly from each other in catalytic activity, which is probably due to their similar ligand backbone. The third monomeric complex used in this study, complex **5**, showed the highest activity for cyclooctene epoxidation, reaching quantitative conversion after 4 h. In contrast, trimeric complex **6**, which contains **5** as a subunit (if the coordinated methanol molecule in **5** is ignored), gave full conversion of **S1** only after 24 h reaction time. For **S3** and **S5** a very similar reactivity profile of **6** compared to **5** was observed, hinting towards a certain stability of the trimer in solution. If **6** was to dissociate in three molecules of **5**, the resulting catalyst loading would be 3 mol%, and should therefore display an enhanced catalytic activity. Since this is not observed in the epoxidation with 1 mol% of **6**, it is feasible that the trimeric complex **6** does not dissociate during catalysis.

For the more challenging substrates **S2**-**S5** yields and selectivities were in general lower for all six complexes **1**-**6**. For the epoxidation of 1-octene **S2**, both yields of epoxide as well as selectivity towards epoxide varied significantly. Yields of epoxide between 23% for **2** and 57% for **5** were observed. Whereas **2** showed high selectivity (>99%) towards epoxide, the other five complexes varied between 68 to 96% selectivity, with 2-octanone being the major side product. For all six complexes, catalytic activity decreased after the first 4 h, with only little conversion to epoxide in the next 20 h. For styrene (**S3**) a similar picture compared to other published Mo complexes [6e,41] was observed, with low conversions and selectivity towards epoxide. There are only few examples of catalysts with high selectivity [6e,6g]. For all six complexes **1**-**6**, a maximum selectivity towards styrene oxide of 20% was observed, with phenyl acetaldehyde and benzaldehyde being the two main over-oxidation products observed. Also yields of styrene oxide were low, ranging between only 6% for **3** and 17% for **1**.

Finally, catalytic activities and selectivities for the substrates limonene **S4** and α-terpineol **S5** are also low, with the over-oxidized ketones limonene oxide and carvone being the major side products. For both substrates **S4** and **S5**, a similar activity profile is observed, with a maximum of epoxide yield observed after 4h, after which the yield of epoxide drops again due to over-oxidation by the catalysts used. Overall, the catalytic activities of complexes **1**-**6** compare well to related dioxomolybdenum(VI) complexes investigated under similar conditions [6e].

Table 3. Conversion of substrate (selectivity to epoxide) for complexes **1-6** with TBHP as oxidant.

[%]	**1**	**2**	**3**	**4**	**5**	**6**
cyclooctene, **S1**	>95 (>99)	>95 (>99)	>95 (>99)	>95 (>99)	>95 (>99)[a]	>95 (>99)
1-octene, **S2**	55 (85)	23 (>99)	52 (68)	51 (74)	60 (96)	31 (96)
styrene, **S3**	90 (19)	65 (22)	94 (6)	86 (11)	71 (15)	74 (14)
limonene, **S4**[b]	>95 (18)	>95 (35)	>95 (30)	>95 (25)	>95 (27)	>95 (59)
α-terpineol, **S5**[b]	>95 (26)	>95 (22)	26 (26)	>95 (23)	>95 (25)	>95 (30)

[a] complete conversion after 4 h; [b] conversion of substrate (selectivity to epoxide) after 4h

In a second round of experiments, the more eco-friendly oxidant H_2O_2 was tested under the same conditions as with TBHP. In this case, conversion of substrate to epoxide was only observed with cyclooctene **S1** (Table 4), but no conversions were observed for **S2-5**; this lack of reactivity was also observed for similar molybdenum complexes [42].

Table 4. Conversion of substrate (selectivity to epoxide) for complexes **1-6** with H_2O_2 as oxidant.

[%]	**1**	**2**	**3**	**4**	**5**	**6**
cyclooctene, **S1**	19 (72)	37 (80)	23 (82)	84 (86)	13 (55)	74 (75)

From the data in Table 4, it is evident that the dimeric complex **4** shows the highest activity in cyclooctene (**S1**) epoxidation with H_2O_2 as oxidant. The reason for this enhanced reactivity, especially when compared to dimeric complex **2**, is not clear. While the selectivities for epoxide are similar for these two dimeric complexes, the conversion rate is much higher for **4**; this may be related to **4** being more prone to formation of (active) mononuclear species/catalysts upon reaction with H_2O_2, thus effectively increasing the catalyst loading. The monomeric complexes **1** and **3** show essentially similar catalytic activities, indicating that the substitution pattern on the ligand backbone has only a small effect on catalytic activity for these catalysts.

Finally, comparison with two previously published, structurally related ligands and their respective Mo(VI) complexes is of interest (Figure 7). The Schiff-base ligand H**L4**, functionalized with a pending ethyl-methoxy arm, [6f] coordinates to the dioxo-molybdenum(VI) core in a bidentate, monoanionic fashion, resulting in the mononuclear complex $[MoO_2(\mathbf{L4})_2]$. In addition, the corresponding, reduced Schiff-base ligand H**L5** exhibiting an NH moiety and a pending ethyl-methoxy arm, [6g] coordinates to the dioxo-molybdenum(VI) core in a bidentate, monoanionic fashion, however resulting in the dinuclear, μ-oxo bridged complex $\{[MoO_2(\mathbf{L5})]\}_2(\mu\text{-O})$. Both complexes $[MoO_2(\mathbf{L4})_2]$ and $\{[MoO_2(\mathbf{L5})]\}_2(\mu\text{-O})$ showed excellent selectivities (>98 %) in epoxidation reactions including for the challenging substrates **S2-5** [6f,6g]. This is ascribed to the influence of the pending methoxy substituent which can possibly form hydrogen bonds during the catalytic reaction and which has been predicted to play an important role by DFT calculations [43]. The lack of such a pending donor in the structurally related complexes **1** and **4** for example, may explain the relatively low observed selectivities with substrates **S2-5** (Table 3).

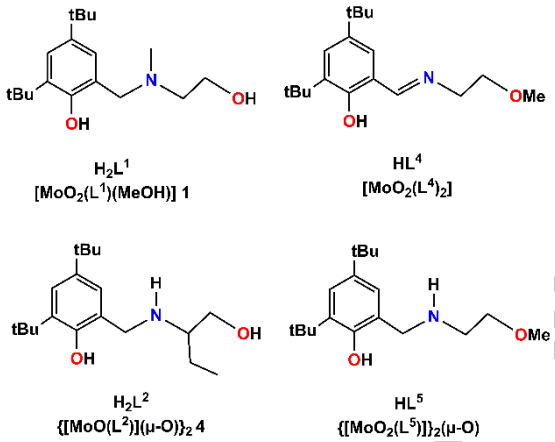

Figure 7. Comparison of structurally related ligands: H_2**L1** and H**L4** [6f]; H_2**L2** and H**L5** [6g].

4. Conclusions

Three mononuclear (**1**, **3**, **5**), two dinuclear (**2**, **4**) and one trinuclear (**6**) molybdenum complexes with tridentate aminoalcohol phenol ligands were synthesised and characterized. All complexes are active and selective catalysts towards the epoxidation of *cis*-cyclooctene using *tert*-butyl hydroperoxide (TBHP) and hydrogen peroxide as oxidants. In addition, all studied complexes showed catalytic activity for more demanding substrates (1-octene, styrene, limonene, α-terpineol) with TBHP as an oxidant, although the conversions and selectivities were generally poor. Complex **6** appears to remain trimeric in solution, judging from the different epoxidation activities in comparison to the analogous monomer **5**. With H_2O_2 as oxidant, the differences in epoxidation activity of **S1** are more pronounced between the six complexes. Complex **4** showed the highest activity with 72% yield of epoxide (conversion x selectivity), whereas **5** gave the lowest yield of epoxide of 7%. The opposite trend was observed for epoxidation with TBHP, where complex **5** was the most active catalyst of all six tested complexes. Stability and solubility in the aqueous media of hydrogen peroxide might be important factors that influence the observed differences in catalytic activity.

Acknowledgements

This paper is dedicated to Rabindranath Mukherjee, a friend, mentor, collaborator and academic leader. We gratefully acknowledge financial support from the COST Action CM1003 *Biological oxidation reactions - mechanisms and design of new catalysts*. M.K.H. thanks the European Commission for the award of an Erasmus Mundus predoctoral fellowship.

Appendix A. Supplementary material

Crystallographic data (excluding structure factors) for the structures in this paper have been deposited with the Cambridge Crystallographic Data Centre, CCDC, 12 Union Road,

Cambridge CB21EZ, UK. Copies of the data can be obtained free of charge on quoting the depository number CCDC 1847230-1847233 (Fax:+44-1223-336-033; E-Mail: deposit@ccdc.cam.ac.uk, http://www.ccdc.cam.ac.uk).

References

1. C. Müller, N. Grover, M. Cokoja, F.E. Kühn, Adv. Inorg. Chem. 65 (2013) 33.
2. (a) A.L. Tenderholt, J.-J. Wang, R.K. Szilagyi, R.H. Holm, K.O. Hodgson, B. Hedman, E.I. Solomon, J. Am. Chem. Soc. 132 (2010) 8359; (b) R. Hille, Chem. Rev. 96 (1996) 2757; (c) R. Hille, Trends Biochem. Sci. 27 (2002) 360; (d) M.J. Romão, Dalton Trans. (2009) 4053; (e) J. Leppin, C. Förster, K. Heinze, Inorg. Chem. 53 (2014) 12416.
3. (a) M. Volpe, N.C. Mösch-Zanetti, Inorg. Chem. 51 (2012) 1440; (b) T. Arumuganathan, M. Volpe, B. Harum, D. Wurm, F. Belaj, N.C. Mösch-Zanetti, Inorg. Chem. 51 (2012) 150.
4. (a) J.M. Mitchell, N.S. Finney, J. Am. Chem. Soc. 123 (2001) 862; (b) C.A. Gamelas, A.C. Gomes, S.M. Bruno, F.A. Almeida Paz, A.A. Valente, M. Pillinger, C.C. Romão, I.S. Gonçalves, Dalton Trans. 41 (2012) 3474.
5. (a) P. Neves, S. Gago, S.S. Balula, A.D. Lopes, A.A. Valente, L. Cunha-Silva, F.A.A. Paz, M. Pillinger, J. Rocha, C.M. Silva, I.S. Gonçalves, Inorg. Chem. 50 (2011) 3490; (b) A.C. Coelho, M. Nolasco, S.S. Balula, M.M. Antunes, C.C.L. Pereira, F.A.A. Paz, A.A. Valente, M. Pillinger, P. Ribeiro-Claro, J. Klinowski, I.S. Gonçalves, Inorg. Chem. 50 (2011) 525.
6. (a) O. Wichmann, R. Sillanpää, A. Lehtonen, Coord. Chem. Rev. 256 (2012) 371; (b) S.K. Kurapati, S. Maloth, S. Pal, Inorg. Chim. Acta 430 (2015) 66; (c) F.E. Kühn, A.M. Santos, M. Abrantes, Chem. Rev. 106 (2006) 2455; (d) M.E. Judmaier, A. Wallner, G. N. Stipicic, K. Kirchner, J. Baumgartner, F. Belaj, N.C. Mösch-Zanetti, Inorg. Chem. 48 (2009) 10211; (e) A. Dupé, M.K. Hossain, J.A. Schachner, F. Belaj, A. Lehtonen, E. Nordlander, N.C. Mösch-Zanetti, Eur. J. Inorg. Chem. (2015) 3572; (f) M.E. Judmaier, C. Holzer, M. Volpe, N.C. Mösch-Zanetti, Inorg. Chem. 51 (2012) 9956; (g) M.E. Judmaier, C.H. Sala, F. Belaj, M. Volpe, N.C. Mösch-Zanetti, New J. Chem. 37 (2013) 2139; (h) N. Zwettler, J.A. Schachner, F. Belaj, N.C. Mösch-Zanetti, Mol. Catal. 443 (2017) 209.
7. (a) M.M. Hänninen, A. Peuronen, P. Damlin, V. Tyystjärvi, H. Kivelä, A. Lehtonen, Dalton Trans. 43 (2014) 14022; (b) X. Lei, N. Chelamalla, Polyhedron 49 (2013) 244; (c) E. Safaei, M. Rasouli, T. Weyhermüller, E. Bill, Inorg. Chim. Acta 375 (2011) 158; (d) E. Laurén, H. Kivelä, M. Hänninen, A. Lehtonen, Polyhedron 28 (2009) 4051; (e) G. Licini, M. Mba, C. Zonta, Dalton Trans. (2009) 5265; (f) S. Padmanabhan, S. Katao, K. Nomura, Organometallics 26 (2007) 1616; (g) H. Sopo, J. Sviili, A. Valkonen, R. Sillanpää, Polyhedron 25 (2006) 1223; (h) Y. Kim, J.G. Verkade, Organometallics 21 (2002) 2395.
8. J. Morlot, N. Uyttebroeck, D. Agustin, R. Poli, ChemCatChem 5 (2013) 601.
9. T. Głowiak, L. Jerzykiewicz, J.M. Sobczak, J.J. Ziółkowski, Inorg. Chim. Acta 356 (2003) 387.
10. A. Lehtonen, R. Sillanpää, Polyhedron 24 (2005) 257.

11. X. Ma, K. Starke, C. Schulzke, H.-G. Schmidt, M. Noltemeyer, Eur. J. Inorg. Chem. (2006) 628.
12. (a) E. Safaei, I. Saberikiaa, A. Wojtczak, Z. Jagličić, A. Kozakiewicz, Polyhedron 30 (2011) 1143; (b) J.C. Ang, Y. Mulyana, C. Ritchie, R. Clérac, C. Boskovic, Aust. J. Chem. 62 (2009) 1124; (c) P.-P. Yang, H.-B. Song, X.-F. Gao, L.-C. Li, D.-Z. Liao, Cryst. Growth Des. 9 (2009) 4064.
13. R. Mayilmurugan, P. Traar, J.A. Schachner, M. Volpe, N.C. Mösch-Zanetti, Eur. J. Inorg. Chem. (2013) 3664.
14. J. Hakala, R. Sillanpää, A. Lehtonen, Inorg. Chem. Commun. 21 (2012) 21.
15. A. Lehtonen, M. Wasberg, R. Sillanpää, Polyhedron 25 (2006) 767.
16. M.M. Hänninen, E. Colacio, A.J. Mota, R. Sillanpää, Eur. J. Inorg. Chem. (2011) 1990.
17. O. Wichmann, A. Lehtonen, Inorg. Chem. Commun. 12 (2009) 15.
18. X. Zhou, Q. Zhang, Y. Hui, W. Chen, J. Jiang, L. Lin, X. Liu, X. Feng, Org. Lett. 12 (2010) 4296.
19. A. Riisiö, O. Wichmann, R. Sillanpää, Lett. Org. Chem. 7 (2010) 298.
20. Rikagu Oxford Diffraction, CrysAlisPro, Agilent Technologies Inc., 2013, Yarnton, Oxfordshire, England.
21. Z. Otwinowski, W. Minor, C.W. Carter, R.M. Sweet, Methods in Enzymol 276 (1997) 307.
22. G.M. Sheldrick, SADABS - Bruker Nonius scaling and absorption correction -, Bruker. AXS, Inc.: Madison, Wisconsin, USA (2012).
23. L. Palatinus, G. Chapuis, J. Appl. Cryst. 40 (2007) 786.
24. G.M. Sheldrick, Acta Crystallogr., Sec C 71 (2015) 3.
25. J.U. Mondal, F.A. Schultz, T.D. Brennan, W.R. Scheidt, Inorg. Chem. 27 (1988) 3950.
26. A. Peuronen, R. Sillanpää, A. Lehtonen, ChemistrySelect 3 (2018) 3814.
27. A. Lehtonen, V. G. Kessler, Inorg. Chem. Commun. 7 (2004) 691.
28. (a) Y.-L. Wong, Y. Yan, E.S.H. Chan, Q. Yang, T.C.W. Mak, D.K.P. Ng, J. Chem. Soc., Dalton Trans. (1998) 3057; (b) (c) Y.-L. Wong, J.-F. Ma, W.-F. Law, Y. Yan, W. T. Wong, Z.-Y. Zhang, T.C.W. Mak, D.K.P. Ng, Eur. J. Inorg. Chem. (1999) 313.
29. M.K. Hossain, M. Haukka, R. Sillanpää, M.G. Richmond, E. Nordlander, A. Lehtonen, Dalton Trans. 46 (2017) 7051.
30. J. Liimatainen, A. Lehtonen, R. Sillanpää, Polyhedron 19 (2000) 1133.
31. C.P. Rao, A. Sreedhara, P.V. Rao, M.B. Verghese, K. Rissanen, E. Kolehmainen, N.K. Lokanath, M.A. Sridhar, J.S. Prasad, J. Chem. Soc., Dalton Trans. (1998) 2383.
32. T.A. Hanna, A.K. Ghosh, C. Ibarra, M.A. Mendez-Rojas, A.L. Rheingold, W.H. Watson, Inorg. Chem. 43 (2004) 1511.
33. S.-J. Mo, B.-K. Koo, Bull. Korean Chem. Soc. 20 (1999) 1105.
34. V. Vrdoljak, J. Pisk, D. Agustin, P. Novak, J.P. Vuković, D. Matković-Čalogović, New J. Chem. 38 (2014) 6176.
35. R. Sillanpää, M.M. Hänninen, Acta Crystallogr., Sec C 69 (2013) 509.
36. H.-Ge. Zhang, Synth. React. Inorg. Met.-Org. Chem. nano-Met. Chem. 43 (2013) 933.
37. L. Ma, R. Jin, Z. Bian, C. Kang, Y. Chen, J. Xu, L. Gao, Chem. Eur. J. 18 (2012) 13168.
38. N.R. Pramanik, S. Ghosh, T.K. Raychaudhuri, R.J. Butcher, S.S. Mandal, J. Coord. Chem. 64 (2011) 1207.

39. J.M. Sobczak, T. Głowiak, J.J. Ziółkowski, Trans. Met. Chem. 15 (1990) 208.
40. E. Salminen, R. Sillanpää, A. Lehtonen, Collect. Czech. Chem. Commun. 75 (2010) 1051.
41. (a) J.A. Schachner, P. Traar, C. Sala, M. Melcher, B.N. Harum, A.F. Sax, M. Volpe, F. Belaj, N.C. Mösch-Zanetti, Inorg. Chem. 51 (2012) 7642; (b) S.A. Hauser, M. Cokoja, F.E. Kühn, Catal. Sci. Technol. 3 (2013) 552; (c) M. Bagherzadeh, L. Tahsini, R. Latifi, L.K. Woo, Inorg. Chim. Acta 362 (2009) 3698; (d) P. Traar, J.A. Schachner, B. Stanje, F. Belaj, N.C. Mösch-Zanetti, J. Mol. Catal. A: Chem. 385 (2014) 54; (e) R. Mayilmurugan, P. Traar, J.A. Schachner, M. Volpe, N.C. Mösch-Zanetti, Eur. J. Inorg. Chem. (2013) 3664.
42. A. Jimtaisong, R.L. Luck, Inorg. Chem. 45 (2006) 10391.
43. (a) A. Comas-Vives, A. Lledós, R. Poli, Chem. Eur. J. 16 (2010) 2147; (b) M.J. Calhorda, P. Jorge Costa, Dalton Trans. (2009) 8155.

Highlights ICA_2018_809

- Six new Mo(VI) oxo complexes have been synthesized and characterized.
- All complexes are based on aminoalcohol phenolate ligands.
- Three complexes are mononuclear, two are dinuclear and one is trinuclear.
- All complexes catalyse epoxidation of olefins by H_2O_2 or ^tBuOOH.

Graphical Abstract